SCIENCE CHINA
Information Sciences

• RESEARCH PAPER •

December 2018, Vol. 61 122202:1–122202:14
https://doi.org/10.1007/s11432-017-9319-0

# Experiment on impedance adaptation of under-actuated gripper using tactile array under unknown environment

Jing CUI[1], Mi LAI[2], Zhongyi CHU[2*] & Fuchun SUN[3]

[1]*School of Mechanical Engineering and Applied Electronics, Beijing University of Technology, Beijing* 100124*, China;*
[2]*School of Instrument Science and Opto-electronics, Beihang University, Beijing* 100191*, China;*
[3]*Department of Computer Science and Technology, Tsinghua University, Beijing* 100084*, China*

Received 3 October 2017/Accepted 30 November 2017/Published online 23 November 2018

**Abstract** The experiment on impedance adaptation to achieve stable grasp for an under-actuated gripper grasping different unknown objects with tactile array is conducted. Under-actuated gripper has a wildly application in the field of space robot and industrial robot because of its better shape-adaptation. However it is difficult to achieve stable grasp owning to the uncertain properties of environment. A control strategy of adaptive matching the impedance parameters is proposed to achieve stable grasp. Firstly, the unknown objects are described as linear systems with unknown dynamics, and the parameters of the object are identified with the recursive least-squares (RLS) method through tactile sensor array. Then a desired impedance model is obtained by defining a cost function that includes the contact force, velocity and displacement errors, and the critical impedance parameters are found to minimize it. Finally, an experiment is presented and shows that the proposed impedance model can guarantee the stable grasp for various unknown objects.

**Keywords** impedance adaptation, under-actuated gripper, tactile array, stable grasp, unknown environment

**Citation** Cui J, Lai M, Chu Z Y, et al. Experiment on impedance adaptation of under-actuated gripper using tactile array under unknown environment. Sci China Inf Sci, 2018, 61(12): 122202, https://doi.org/10.1007/s11432-017-9319-0

## 1 Introduction

In recent years, the control design and stability analysis of robot have received considerable attention, and the control system of the robotic manipulator has been developed during the past decade, such as education, entertainment and rehabilitation. Thereinto, under-actuated gripper is one of the most popular robotic manipulator, which has a wild application in the field of space robot and industrial robot because of its better shape-adaptation [1]. In the field of space robot, some researchers focus on the tether space robot [2, 3]. Huang et al. [4] proposed a robust control method based on back stepping control method to deal with the stabilization problem of the tether space robot. The control stability of the tether space robot was further studied by [5]. In the field of industrial robot, some researchers combined the visual and tactile sensing for robotic stable grasp [6–9]. However, in the most cases, the parameters of the grasped object are unknown, which is difficult to achieve stable grasp owning to the uncertain properties of environment. The balance between the contact force and the input torque attributes to the stable

* Corresponding author (email: chuzystar@gmail.com)

 

grasp, so a proper contact force is essential for the grasp of under-actuated gripper. It is valuable to mention that, the contact force cannot directly be obtained. It can be adjusted by controlling the input torque based on the balance between the contact force and the input torque. Thus, it can be seen that the input torque is associated with the properties of environment [10], so it is important to identify the unknown parameters of the object to achieve proper contact force [11, 12] in the interaction between robots and environment.

In the field of interaction control, position/force hybrid controller is a classic processing method [13]. However, this method usually cannot control the dynamic characteristics of the finger, which is difficult to ensure compliant grasp. Then Hogan [14] proposed impedance control, which is now the most popular control method because of its better robustness [15–18]. However, the model parameters of traditional impedance controller are constant, which will lead to insufficient adaptability. Therefore some researchers have done further studies including adaptive impedance control and learning impedance control. Learning impedance control has been used to achieve impedance parameters in unknown environment. For example Petkovic et al. [19] designed an adaptive neural fuzzy controller with impedance parameters self-adjusting mechanism, but its computational complexity limits the application in practice. A grasp adaptation strategy which does not depend on the specific impedance model was proposed in [20, 21] to perform robust grasping, but the effect is closely related to the prior experience, and the robustness is difficult to guarantee. A novel policy iteration approach which does not require prior knowledge of system was proposed in [22], however it is only for state regulation. It can be acknowledged that learning impedance control requires the robot to repeat operations to learn desired impedance parameters that will easily cause inconvenience.

For adaptive impedance control, optimization is important because the control objective of impedance control contains force regulation and trajectory tracking. Johansson et al. [23] has done related work to define an optimization function that includes contact force and position deviation. The desired impedance parameters are obtained by minimizing the optimization function. However, the kinetic parameters of the environment are known. Adaptive dynamic programming (ADP) is developed to achieve optimal control in the case of unknown system. Xu et al. [24] studied the control of a flexible-link manipulator with uncertainty; the sliding mode control was proposed while the adaptive design was developed using neural networks (NNs). He et al. [25] investigated adaptive fuzzy neural network (NN) control using impedance learning for a constrained robot, which does not need the prior knowledge of the uncertainty and a sufficient amount of observed data. In [26], adaptive impedance control was developed for an $n$-link robotic manipulator with input saturation by employing neural networks. Whatever to say, the above methods require the robot repeating the same motion to obtain the desired impedance parameters, which consumes a lot of energy [27,28]. To solve this problem, Ref. [29] proposed an adaptive impedance control method that achieves the adaptive adjustment of the parameters by minimizing the linear cost function, however the impedance model of the unknown environment is still based on strict linear assumption. Although impedance adaptation has been widely developed, it is difficult to realize stable control based on the identification of the unknown object, because it is impossible to control the position of each phalanx independently for under-actuated gripper.

This paper presents a control strategy of adaptive impedance parameters matching on a three-finger under-actuated gripper using tactile sensor array to achieve stable grasp under unknown environment. Firstly, the unknown objects are described as linear systems with unknown dynamics, which is described as a mass-damping-stiffness system. The parameters of the object are identified with the recursive least-squares (RLS) method using the tactile sensor array and a state function is established with the identified parameters. Then, a desired impedance model is obtained by defining a cost function that includes the contact force, velocity and displacement errors. Owning to the under-actuated characteristics, it is difficult to directly measure each phalanx's displacement and it can be obtained through the geometric relationship with measured joint angles. Finally, the critical impedance parameters are found to minimize the cost function and the desired impedance model is imposed to the under-actuated gripper to achieve stable grasp.

This paper is organized as follows. The mechanism and experimental setup are introduced in Section 2.

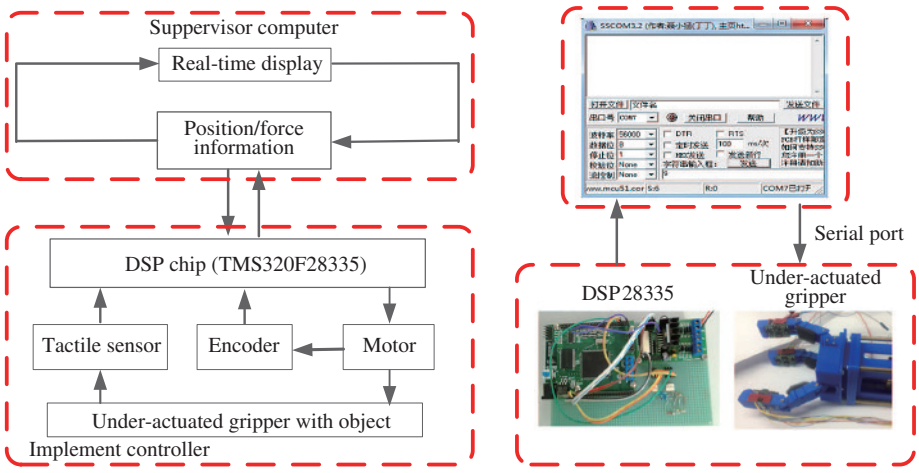


**Figure 1** (Color online) The scheme of experimental system.

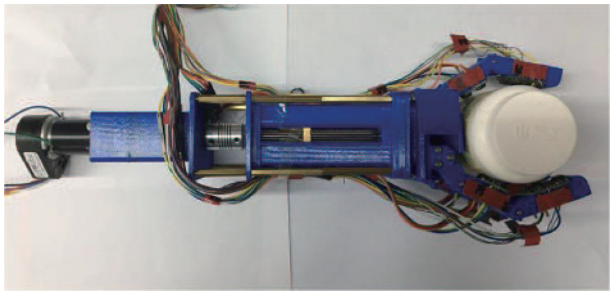

**Figure 2** (Color online) The structure of under-actuated gripper system.

In Section 3, the impedance adaptive control and the identification of environment parameters are presented. The availability of the proposed method is verified through experiments in Section 4. Section 5 concludes the paper.

## 2 Mechanism and experimental setup

The experimental system includes a supervisor computer and an implementation controller as shown in Figure 1. The implementation controller consists of the under-actuated gripper system and the hardware control architecture. The main chip of the hardware control circuit is the DSP28335 which controls the grasp action of the under-actuated gripper, and the motor is driven by PWM mode. The DSP28335 also collects the motor rotation and tactile sensing information, and then sends them to the supervisor computer through the serial port. The supervisor computer displays the measurements based on the serial debugging software, and its main function is to send control instructions, and to display the information in real time which is transmitted by the DSP28335.

### 2.1 Mechanism

The structure of the under-actuated gripper system is shown in Figure 2, which consists of three parts: the driving portion, the gripper portion and the tactile sensor. The driving portion consists of one driving motor, one slider and one screw. The gripper portion consists of three under-actuated fingers with rotational springs, i.e., passive actuators. The detailed construction of the under-actuated gripper finger is shown in Figure 3. The gripper has three fingers. Each finger has two knuckles, the proximal knuckle and the distal knuckle. The tactile sensor array is fixed on the fingers to measure the contact force.

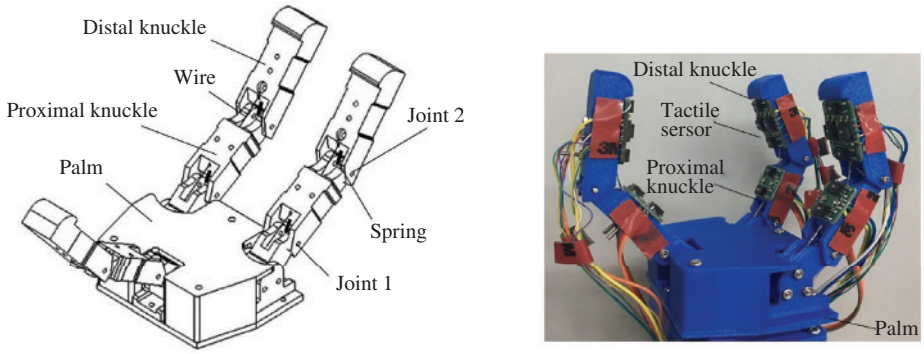


**Figure 3** (Color online) The construction of the under-actuated gripper finger.

**Table 1** The geometric size of under-actuated gripper

| | Length (mm) | Width (mm) | Thickness (mm) |
|---|---|---|---|
| Proximal knuckle | 40 | 18 | 15 |
| Distal knuckle | 50 | 18 | 15 |
| Palm | 80 | 60 | – |

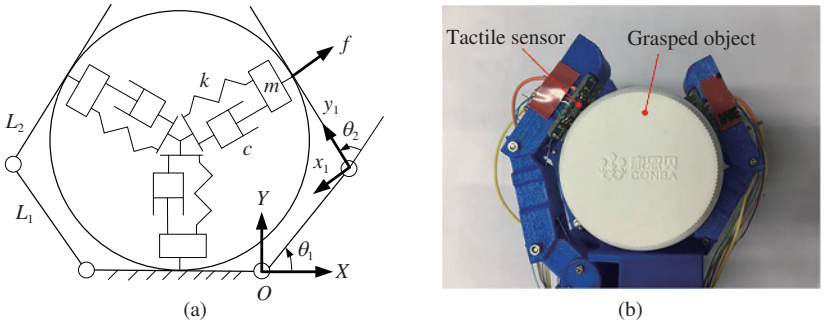


**Figure 4** (Color online) The under-actuated gripper with an unknown grasped object. (a) The model of gripper and object; (b) the under-actuated gripper with an unknown grasped object.

The under-actuated gripper is designed according to the size of the human finger, and the specific parameters are shown in Table 1. In particular, the surface of the finger is integrated with the tactile sensor array, so the thickness given in the table is the total thickness of the finger with the sensor array.

## 2.2 Model

When the under-actuated gripper grasps an unknown object in the experiment, the model is shown in Figure 4 [30]. It can be seen from Figure 4(a) that the unknown environment is described as a mass-damping-stiffness system with unknown environmental parameters such as contact mass, damping and stiffness [28].

The dynamic equation of the unknown grasped object is

$$f = -m\ddot{x} - 2C\dot{x} - 2Kx, \tag{1}$$

where $\ddot{x}, \dot{x}$ and $x$ are the acceleration, velocity and displacement of the contact point, respectively, which change along the $x_1$ axis. $f$ is the contact force between the object and the knuckle, which can be measured by a tactile sensor. $m, C$ and $K$ are the unknown environmental parameters, which are related to the contact mass, damping and stiffness. The state function of a mass-damping-stiffness system is described as

$$\dot{\xi} = \boldsymbol{A}\xi + \boldsymbol{B}\boldsymbol{u}, \tag{2}$$

where $\boldsymbol{u}$ is the system input which is chosen as $\boldsymbol{u} = [f]$, $\xi$ is the system state which is chosen as $\xi = [\dot{x} \;\; x \;\; z]^{\mathrm{T}}$, and $\boldsymbol{A}$ and $\boldsymbol{B}$ are unknown constant matrices related to the parameters of grasped object

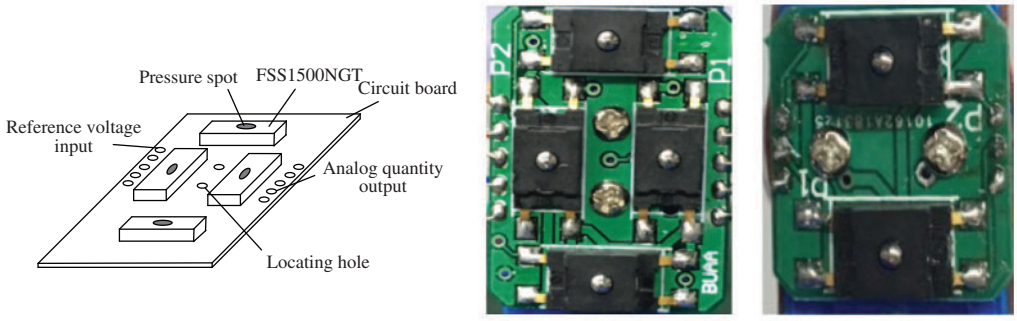


(a) (b) (c)

**Figure 5** (Color online) The sensor array. (a) The structure of sensor array; (b) $2 \times 2$ sensor array; (c) $2 \times 1$ sensor array.

($m$, $C$ and $K$). $z \in \mathbb{R}^m$ is the state of the following system [23]:

$$\begin{cases} \dot{\boldsymbol{Z}} = \boldsymbol{U}\boldsymbol{Z}, \\ x_t = \boldsymbol{V}\boldsymbol{Z}, \end{cases} \tag{3}$$

where $\boldsymbol{U} \in \mathbb{R}^{m\times m}$ and $\boldsymbol{V} \in \mathbb{R}^{n\times m}$ are known constant matrices. Substituting (1) into (2), the state function can be written as

$$\begin{bmatrix} \ddot{x} \\ \dot{x} \\ x \end{bmatrix} = \begin{bmatrix} -2\boldsymbol{C}m^{-1} & -2\boldsymbol{K}m^{-1} & 0 \\ \boldsymbol{I} & 0 & 0 \\ 0 & 0 & \boldsymbol{U} \end{bmatrix} + \begin{bmatrix} -m^{-1} \\ 0 \\ 0 \end{bmatrix} f, \tag{4}$$

$$\boldsymbol{A} = \begin{bmatrix} -2\boldsymbol{C}m^{-1} & -2\boldsymbol{K}m^{-1} & 0 \\ \boldsymbol{I} & 0 & 0 \\ 0 & 0 & \boldsymbol{U} \end{bmatrix}, \quad \boldsymbol{B} = \begin{bmatrix} -m^{-1} \\ 0 \\ 0 \end{bmatrix}. \tag{5}$$

The desired impedance model in impedance adaptive control is based on the state function of unknown grasped object, which will be introduced in detail in Section 3.

### 2.3 Sensor array

In order to achieve the stable grasp of under-actuated gripper, it is necessary to measure the contact force between the fingers and the object, which makes the gripper take an appropriate grasp force. Tactile sensor is generally used for measuring contact force. A single tactile sensor has limitations in the measurement. It can only measure a certain point or a local range of pressure. Therefore a sensor array which can integrate multiple tactile sensors is proposed. It can measure not only the contact force, but also the contact position between the fingers and the object, where the maximum pressure outputs. The numbers of pressure spots in the sensor array are designed as $2 \times 2$ and $2 \times 1$ in this paper, which are fixed on the distal knuckle and proximal knuckle respectively. The pressure spot are FSS1500NGT force sensors which are installed in the illustrated position, as shown in Figure 5.

The static characteristic of sensor array are tested by experiments, the sensor is arranged on a horizontal platform, and the output of the sensor array is measured with the loading change from 0 to 2000 g with a 100-g step length. The measurement result and the fitting curve obtained from recursive-least-squares (RLS) are shown in Figure 6. It can be seen that the fitting curve is close to the measurement result. The error between the fitting value and the measured value is shown in Figure 7, and the maximum value is less than 1.5 mV.

The loading test is repeated on the sensor array for twice, and the result of the 1st and the 2nd measurements are very similar as shown in Figure 8. The difference between the two measurements is shown in Figure 9 and the maximum value is less than 0.6 mV.

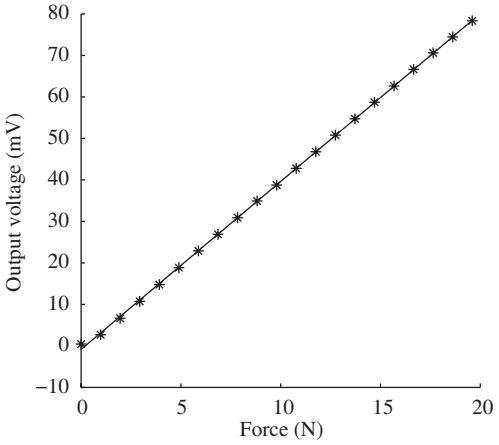


**Figure 6** The static characteristic of sensor.

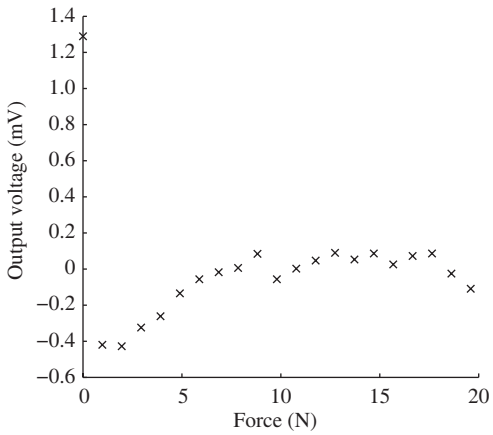


**Figure 7** The error between the fitting value and the measured value.

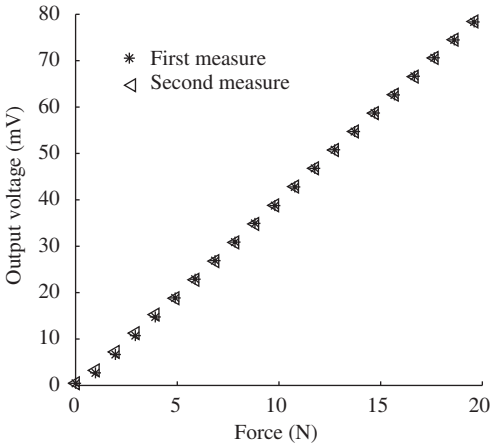


**Figure 8** The repeated test on the sensor array.

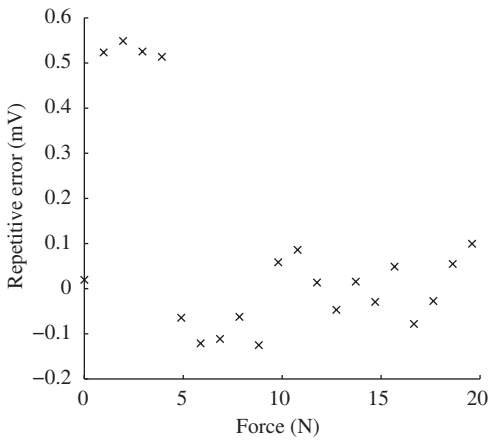


**Figure 9** The error of repeated test.

The positive and negative loading process is also tested on the sensor array. The positive process is loaded from 0 to 2000 g with a 100-g step length; the negative process is also loaded from 2000 to 0 g, with a 100-g step length. The loading results are shown in Figure 10. The error between positive and negative process is different, as shown in Figure 11.

The performance of the sensor array depends on the performance of the FSS1500NGT sensor, and it is tested and shown in Table 2. It can be seen that the sensor array has good linearity, repeatability and hysteresis.

## 3 Impedance adaptive control scheme

In this section, we describe our approach to learn parameters of the unknown object based on tactile sensing information and apply it to the impedance adaptive control. The proposed impedance adaptive control scheme of the system is shown in Figure 12, which includes the identification of object parameters and desired impedance model.

### 3.1 Identification of the unknown grasped object based on RLS

Identification of the unknown environment parameters based on RLS is briefly introduced in this subsection. The results will be used for the development of the impedance adaptation. Recalling (1), for each

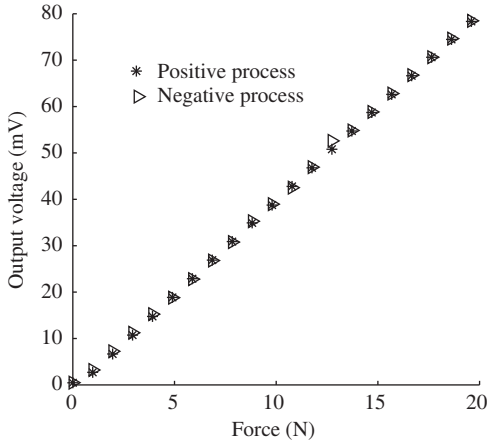


**Figure 10** The positive and negative loading process on the sensor array.

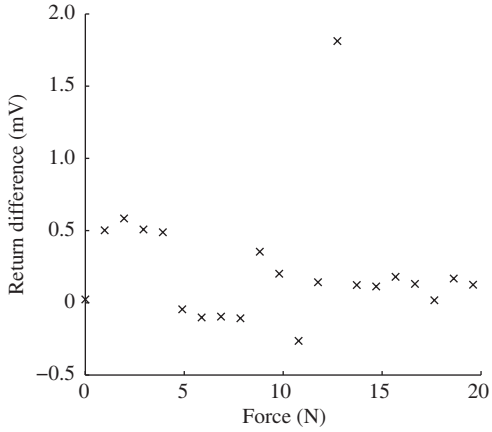


**Figure 11** The return difference.

**Table 2** The performance of sensor array

| Item | Value |
|---|---|
| Linearity | 1.64% |
| Sensitivity | 4.05 mV/N |
| Repetition rate | 0.70% |
| Thickness | 5 mm |
| Total area | 30 mm × 18 mm |
| Temperature range | $-40°-+85°$ |

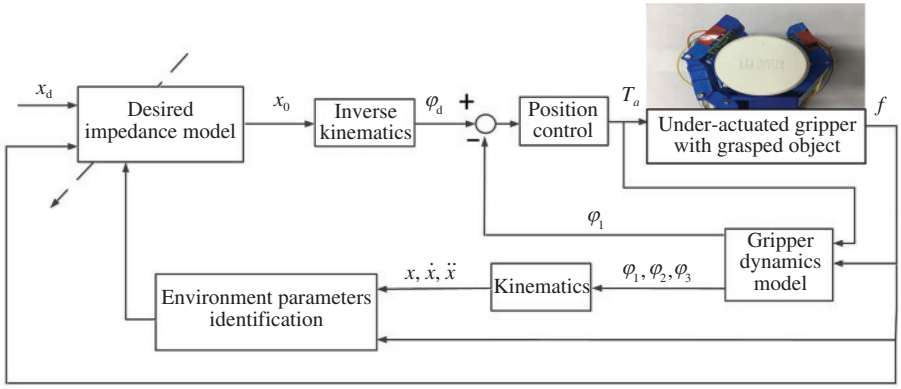


**Figure 12** (Color online) Schematic of the impedance adaptive control.

$k \in \mathbb{Z}^+$ where $k$ stands for $k$th and $\mathbb{Z}^+$ is positive integer set, the discretization of (1) is

$$f(k) = -m\ddot{x}(k) - 2C\dot{x}(k) - 2Kx(k). \tag{6}$$

Eq. (6) can be rewritten as matrix form as

$$\boldsymbol{f}(k) = -\boldsymbol{r}^{\mathrm{T}}(k)\boldsymbol{w}, \tag{7}$$

where

$$\boldsymbol{r}(k) = [\ddot{x}(k) \;\; 2\dot{x}(k) \;\; 2x(k)]^{\mathrm{T}}, \tag{8}$$

$$\boldsymbol{w} = [m \;\; \boldsymbol{C} \;\; \boldsymbol{K}]^{\mathrm{T}}. \tag{9}$$

$\boldsymbol{w}$ is estimated through RLS method [31]:

$$\hat{\boldsymbol{w}}(t) = \hat{\boldsymbol{w}}(t-1) + \boldsymbol{L}((t))[\boldsymbol{f}(t) - \boldsymbol{r}^{\mathrm{T}}(t)\hat{\boldsymbol{w}}(t-1)], \tag{10}$$

where

$$\boldsymbol{L}((t)) = \boldsymbol{P}(t-1)\boldsymbol{r}(t)[1+\boldsymbol{r}^{\mathrm{T}}(t)\boldsymbol{P}(t-1)\boldsymbol{r}(t)]^{-1}, \tag{11}$$

$$\boldsymbol{P}(t) = [\boldsymbol{I}_3 - \boldsymbol{L}(t)\boldsymbol{r}^{\mathrm{T}}(t)]\boldsymbol{P}(t-1). \tag{12}$$

In (11) the variable $\boldsymbol{P}(t)$ is the covariance matrix whose size is $3\times 3$, and $\boldsymbol{P}(0) = p_0\boldsymbol{I}_3$, where $p_0$ is a large positive number, e.g., $p_0 = 10^6$. The estimation error is defined as $\delta = \hat{w}(t) - w$, which approaches zero when the input signal is persistently excited with finite variance, and the noise has a zero mean. Thus, the parameters of grasped object-contacting inertia $m$, damping $C$ and stiffness $K$ are obtained using the RLS algorithm.

### 3.2 Impedance adaptive control

$T_a$ in the schematic is the driving torque exerted by motor and $f$ is the contact force between the fingers and the object. The desired impedance model is defined as

$$f = Z(x_0, x_{\mathrm{d}}), \tag{13}$$

where $Z(\cdot)$ is a target impedance function that needs to be determined, $x_{\mathrm{d}}$ is the desired trajectory of the contact point, and $x_0$ is the virtual desired trajectory. Assume $x_0(t) = x(t)$ for an ideal position controller. The desired impedance model can be rewritten as

$$f = Z(x, x_{\mathrm{d}}). \tag{14}$$

It is worth mentioning that $Z(\cdot)$ is based on the unknown grasped object. A cost function that includes contact force, position deviation, and velocity is defined to solve $Z(\cdot)$, which is expressed as follows [32]:

$$\begin{aligned}\Gamma &= \int_0^{+\infty} \left(\dot{x}^{\mathrm{T}}Q_1\dot{x} + (x-x_{\mathrm{d}})^{\mathrm{T}}Q_2(x-x_{\mathrm{d}}) + f^{\mathrm{T}}rf\right)\mathrm{d}t \\ &= \int_0^{+\infty} \left(\dot{x}^{\mathrm{T}}Q_1\dot{x} + \begin{bmatrix}x^{\mathrm{T}} & \boldsymbol{z}^{\mathrm{T}}\end{bmatrix}\begin{bmatrix}Q_2' & -Q_2'V \\ -V^{\mathrm{T}}Q_2' & V^{\mathrm{T}}Q_2'V\end{bmatrix}\begin{bmatrix}x \\ z\end{bmatrix} + f^{\mathrm{T}}rf\right)\mathrm{d}t \\ &= \int_0^{+\infty} [\xi^{\mathrm{T}}Q\xi + f^{\mathrm{T}}Rf]\mathrm{d}t.\end{aligned} \tag{15}$$

In (15), $\boldsymbol{Q}$ and $\boldsymbol{R}$ are the weighting matrices which satisfy

$$\boldsymbol{Q} = \boldsymbol{Q}^{\mathrm{T}} = \begin{bmatrix}Q_1 & 0 & 0 \\ 0 & Q_2' & -Q_2'\boldsymbol{V} \\ 0 & -\boldsymbol{V}^{\mathrm{T}}Q_2' & \boldsymbol{V}^{\mathrm{T}}Q_2'\boldsymbol{V}\end{bmatrix}, \quad \boldsymbol{R} = [r], \tag{16}$$

where $Q_1$ and $Q_2'$ are factors: $Q_1 \geqslant 0$, $Q_2' \geqslant 0$ and $r \geqslant 0$. For certain $\boldsymbol{Q}$ and $\boldsymbol{R}$, solve the following Riccati equation:

$$\boldsymbol{P}\boldsymbol{A} + \boldsymbol{A}^{\mathrm{T}}\boldsymbol{P} - \boldsymbol{P}\boldsymbol{B}\boldsymbol{R}^{-1}\boldsymbol{B}^{\mathrm{T}}\boldsymbol{P} + \boldsymbol{Q} = 0. \tag{17}$$

The optimal feedback gain matrix can be obtained:

$$\boldsymbol{K}_k = -\boldsymbol{R}^{-1}\boldsymbol{B}^{\mathrm{T}}\boldsymbol{P}. \tag{18}$$

We define that

$$\boldsymbol{P} = \begin{bmatrix}\boldsymbol{P}_1 & \boldsymbol{P}_2 & \boldsymbol{P}_3 \\ \star & \star & \star \\ \star & \star & \star\end{bmatrix}, \tag{19}$$

where $\boldsymbol{P}_1 \in \mathbb{R}^{n\times n}$, $\boldsymbol{P}_2 \in \mathbb{R}^{n\times n}$ and $\boldsymbol{P}_3 \in \mathbb{R}^{n\times n}$, and $\star$ represents the elements that do not concern this problem. Then, the desired impedance model has been obtained according to $\boldsymbol{K}_k$ and the optimal control states (Eq. (5)):

$$f = -\boldsymbol{K}_k\xi = -\boldsymbol{R}^{-1}\boldsymbol{B}^{\mathrm{T}}\boldsymbol{P}\xi. \tag{20}$$


**Figure 13** (Color online) The unknown grasped objects.

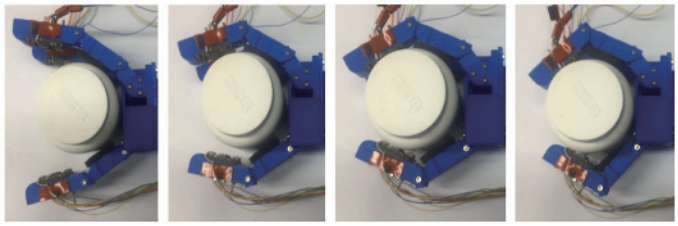


**Figure 14** (Color online) The unknown grasped objects. (a) Initial state; (b) close state; (c) contact state; (d) grasp state.

By substituting (19) into (20), we can obtain desired impedance model

$$\begin{aligned} f &= m^{-1}\mathbb{R}^{-1}\boldsymbol{P}_1\dot{x} + m^{-1}\mathbb{R}^{-1}\boldsymbol{P}_2 x - m^{-1}\mathbb{R}^{-1}\boldsymbol{P}_3 z \\ &= m^{-1}\mathbb{R}^{-1}(\boldsymbol{P}_1\dot{x} + \boldsymbol{P}_2 x - \boldsymbol{P}_3\boldsymbol{V}^{\mathrm{T}}(\boldsymbol{V}\boldsymbol{V}^{\mathrm{T}}))^{-1}x_{\mathrm{d}} \\ &= -k_0\ddot{x} - k_1 x - k_2 x_{\mathrm{d}}. \end{aligned} \tag{21}$$

$k_0$, $k_1$ and $k_2$ can be obtained by solving the Riccati equation under certain $\boldsymbol{A}$, $\boldsymbol{B}$, $\boldsymbol{Q}$ and $\boldsymbol{R}$:

$$k_0 = -\sqrt{Q_1^2/r - 2mk_1 + 4C^2} + 2C, \tag{22}$$

$$k_1 = -\sqrt{Q_2'/r + 4K^2} + 2K, \tag{23}$$

$$k_2 = Q_2'\boldsymbol{V}r^{-1}(k_0\boldsymbol{U} - 2C\boldsymbol{U} + m\boldsymbol{U}^2 + 2\boldsymbol{K}\boldsymbol{I} - k_1\boldsymbol{I})^{-1}\boldsymbol{V}^{\mathrm{T}}(\boldsymbol{V}\boldsymbol{V}^{\mathrm{T}})^{-1}. \tag{24}$$

Therefore, the desired impedance model with the measurement of $\boldsymbol{f}$, $\boldsymbol{x}$ and $x_{\mathrm{d}}$ can be obtained, as shown in (21).

## 4 Experiments

### 4.1 Experimental conditions

In the experiments, four different materials are used to verify the stability of the impedance adaptive control, including plastic bottle, water bottle, glass cup and insulation cup named as object 1, 2, 3, and 4, respectively, as shown in Figure 13.

A complete grasp process is shown in Figure 14. At the beginning, the under-actuated gripper is open, as shown in Figure 14(a). Then the under-actuated gripper gradually approaches to the object (Figure 14(b)) until it contacts (Figure 14(c)) and grasps (Figure 14(d)) the object stably. The weighting matrices are chosen as $Q_1 = 1$, $Q_2' = 3000 \times 3000$ and $r = 1$ in the experiment. The matrices $\boldsymbol{U}$ and $\boldsymbol{V}$

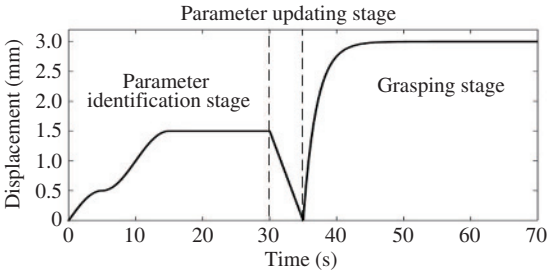


**Figure 15** The desired trajectory.

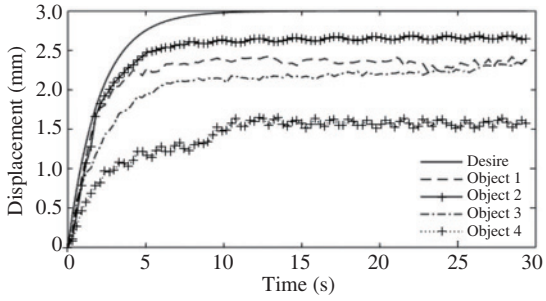


**Figure 16** The displacement experimental results.

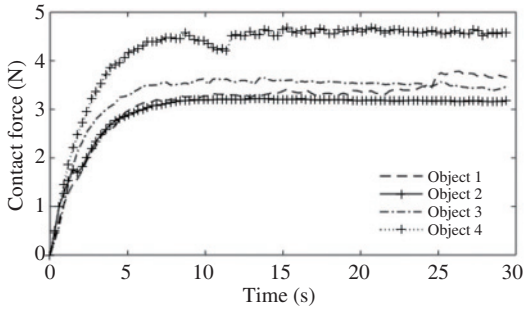


**Figure 17** Contact force experimental results.

are chosen as $\boldsymbol{U} = \left[\begin{smallmatrix} 0 & -1 \\ 0 & 0.5 \end{smallmatrix}\right]$ and $\boldsymbol{V} = [1 \;\; 0.01]$. The position control is achieved by the PID controller, which is used to ensure trajectory tracking in joint space, and the parameters are chosen as $P = 20$, $I = 3$, and $D = 0$. The desired trajectory in the experiment is shown in Figure 15, which is divided into the parameter identification stage, the parameter updating stage and the grasping stage. In the parameter identification stage, the regular contact trajectory is a section function. Position control is applied in this stage so that the contact point can track the desired trajectory, which is used to identify the contact mass, damping and stiffness of the unknown object. It is also used to calculate the parameters of the desired impedance model in real time. Because the parameters of the object are unknown, the larger contact displacement may damage the object or the gripper, so it is necessary to select the appropriate desired trajectory in the identification stage. Therefore, the maximum contact displacement is designed to be 1.5 mm which will not damage the object and gripper even in the case of objects with large rigidity. The impedance model $f = -\boldsymbol{K}_0\xi$ is applied to the control system, where $K_0 = [1 \;\; 1000 \;\; 1000]$ is the initial value of the impedance parameters. In the parameter updating phase, the identification of parameters has been completed and the parameters of the desired impedance model are also calculated according to (21)–(23). The under-actuated gripper is returned to the initial contact state for preparation. The desired trajectory is designed to be $x_{\mathrm{d}} = 3 - 3\mathrm{e}^{-0.5t}$. In the grasping tage, as shown in Figure 15, the impedance model for this period is $f = \dot{x} - 2656x + 4435x_{\mathrm{d}}$. The impedance parameters are used to update the impedance model, and the under-actuated gripper will perform adaptive grasping process according to the parameters of the object.

### 4.2 Experimental results

The experimental results are shown in Figures 16 and 17. Figure 16 shows the contact displacement and Figure 17 shows the contact force during the grasp. It can be seen that the contact displacement and force tend to stable after 10 s. The difference of stable displacement and contact force also shows the corresponding adaptability according to the different object. It can be seen from Figure 16 that the contact displacement of the object 2 is the largest, followed by the object 1, object 3 and object 4. The displacements, which are 2.6, 2.4, 2.1 and 1.5 mm, respectively, coincide with the hardness of the four objects. It can be explained that the deformation will be larger when the grasped object has smaller

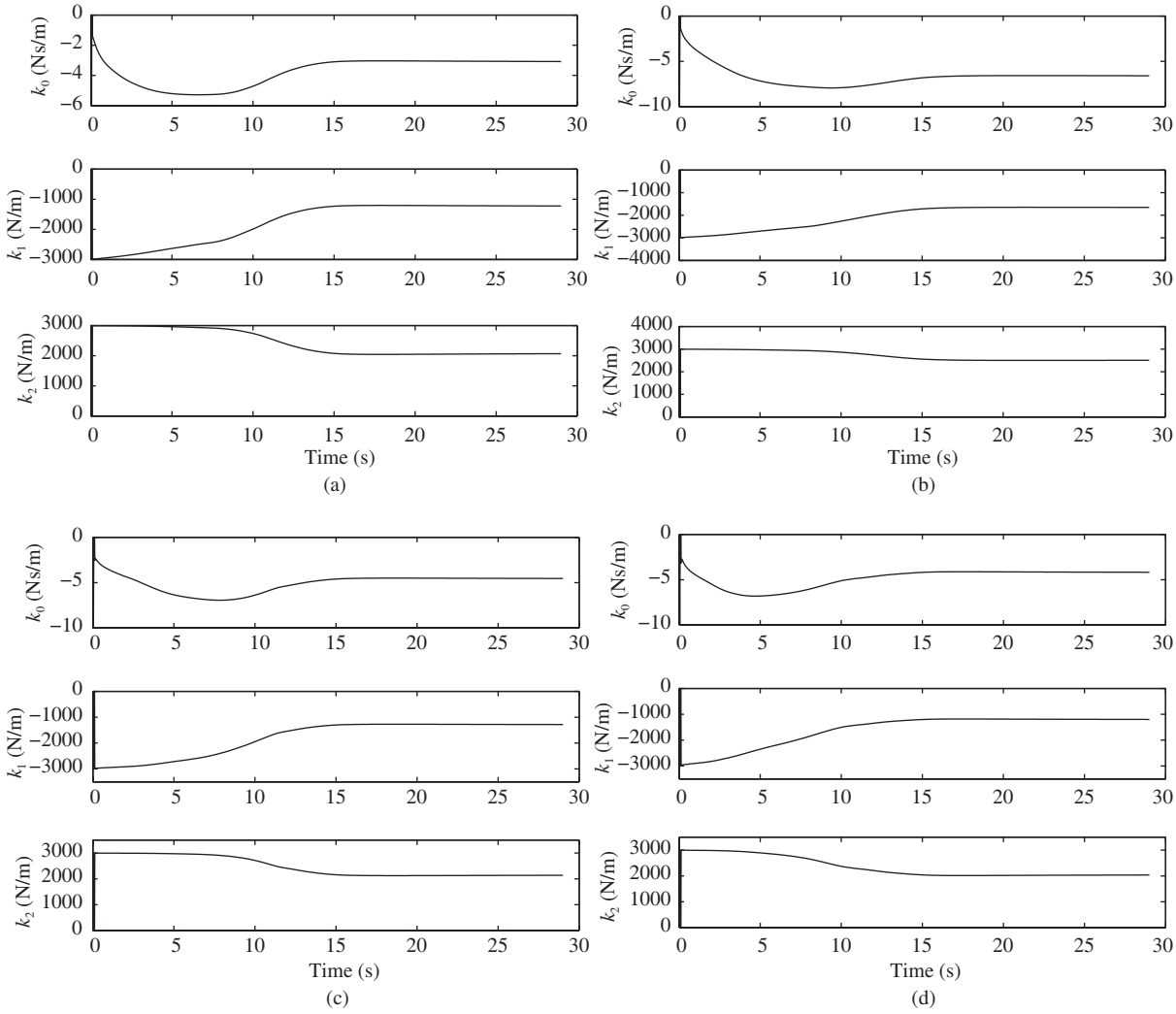


**Figure 18** The parameters of desired impedance model. (a) Object 1; (b) object 2; (c) object 3; (d) object 4.

**Table 3** The parameters of desired impedance model (steady-state value)

| Object | $k_0$ (Ns/m) | $k_1$ (N/m) | $k_2$ (N/m) |
|---|---|---|---|
| Object 1 | −3.0 | −1217.3 | 2057.1 |
| Object 2 | −6.4 | −1648.3 | 2502.7 |
| Object 3 | −4.6 | −1275.6 | 2129.5 |
| Object 4 | −4.0 | −1189.6 | 2024.6 |

stiffness value. On the contrary, for the stiffer objects, the deformation will be relatively smaller. The contact force (in Figure 17) also shows the same rule. When the object 2 is grasped, the contact force is 3 N, and the contact force is 4.6 N for the object 4. It requires a larger contact force to achieve stable grasp for an object with larger stiffness value.

The experiments demonstrate the self-adaptability. It can be seen that the under-actuated gripper achieves stable grasp with four different objects, and the displacement and the contact force are both various for different objects. This adaptation depends on the parameters of the impedance controller and the parameters become stable after 15 s, as shown in Figure 18. The details of the parameters are shown in Table 3.

It is expected that the resolution and updating of the impedance parameters are based on the identification of the object parameters, so the accuracy of the parameter estimation affects the stability of the grasp. The estimation of the object parameters in the identification is shown in Figure 19.

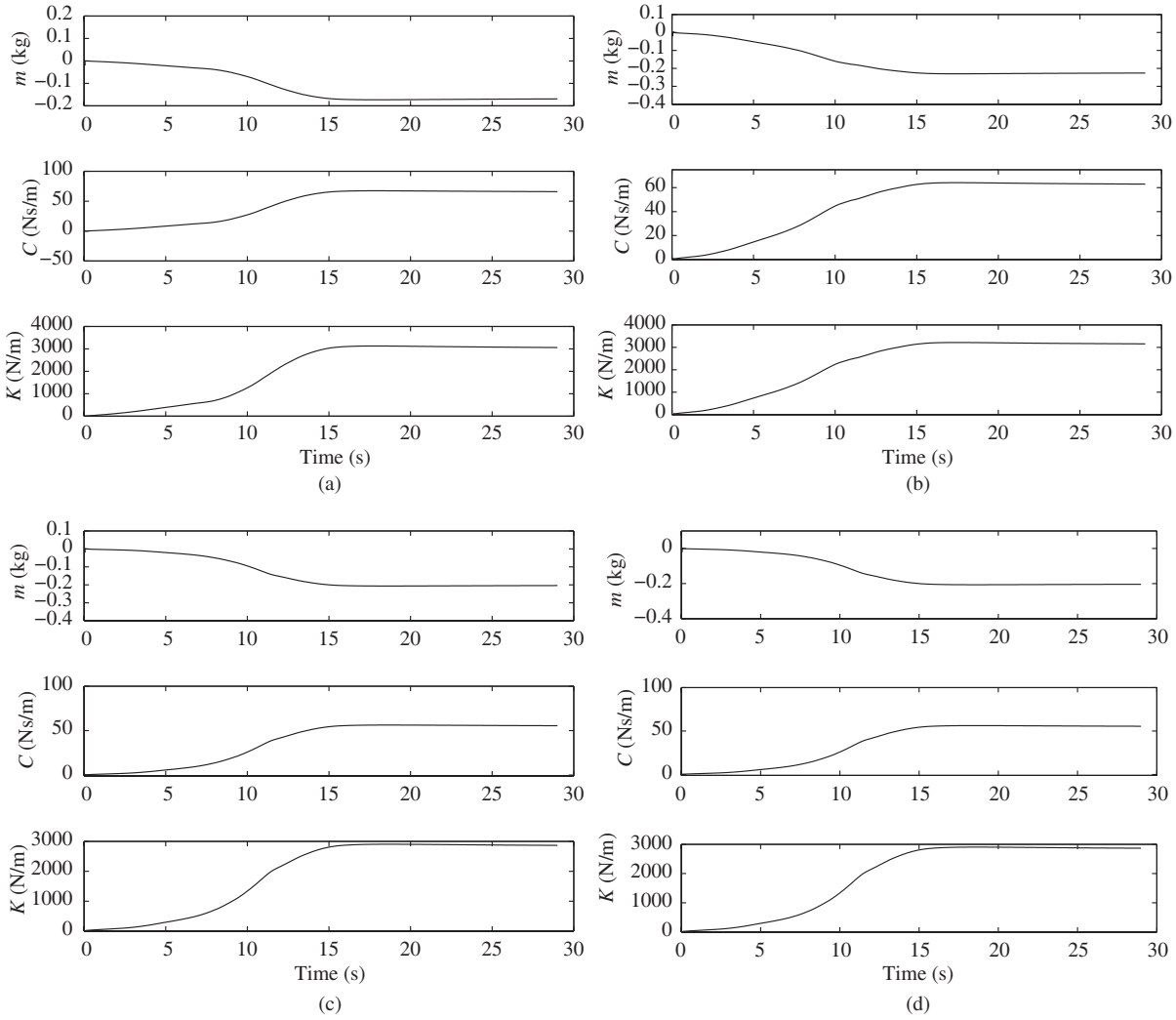


**Figure 19** The parameters of unknown objects. (a) Object 1; (b) object 2; (c) object 3; (d) object 4.

From Figure 19, it can be seen that the change of the object parameters is similar to the change of desired impedance parameters, and the estimated value of the object parameters reach steady after 15 s, which verifies the effective of recursive least squares (RLS) method. The steady-state values of the desired impedance parameters and unknown objects are shown in Table 3. In this experiment, the under-actuated gripper can achieve stable grasp for four different objects with various impedance model parameters to verify self-adaptability of the system. Therefore, the results show that the proposed impedance adaptive control method is effective and feasible.

## 5 Conclusion

In this paper, the impedance adaptation has been developed to achieve stable grasp for an under-actuated gripper grasping different objects with tactile array, based on the desired impedance model which has been obtained to match the unknown objects. The unknown grasped object is described as a mass-damping-stiffness system, and the parameters of the object are identified with the recursive-least-squares (RLS) method through tactile sensor array. Then a desired impedance model is obtained by defining a cost function that includes the contact force, velocity and displacement errors, and the critical impedance parameters are found to minimize it. Finally, the desired impedance model is imposed to the under-actuated gripper to achieve a stable grasp. The experiment shows that the proposed impedance model

can guarantee the stability of grasp, and also present adaptation for various objects.

The method proposed in this paper is based on the identification of object parameters, the contacting inertia $m$, stiffness $K$ and damping $C$ are obtained from the recursive-least-squares (RLS). However, it is difficult to measure the theoretical characteristic of the actual object, so further study is needed to verify the accuracy of the characteristic identification. Our future work will also focus on the measurement of under-actuated gripper's joint angles, which can improve the identified accuracy of unknown objects.

**Acknowledgements** This work was supported by National Natural Science Foundation of China (Grant Nos. 61773028, 51375034), Natural Science Foundation of Beijing (Grant No. 4172008), and the Fundamental Research Funds for the Central Universities (Grant No. YWF-17-BJ-J-78).

## References

1 Kragten G A, van der Helm F C T, Herder J L. A planar geometric design approach for a large grasp range in underactuated hands. Mechanism Machine Theor, 2011, 46: 1121–1136
2 Huang P F, Wang D, Meng Z, et al. Impact dynamic modeling and adaptive target capturing control for tethered space robots with uncertainties. IEEE/ASME Trans Mechatron, 2016, 21: 2260–2271
3 Wang D, Huang P F, Meng Z. Coordinated stabilization of tumbling targets using tethered space manipulators. IEEE Trans Aerospace Electron Syst, 2015, 51: 2420–2432
4 Huang P F, Wang D, Zhang F, et al. Postcapture robust nonlinear control for tethered space robot with constraints on actuator and velocity of space tether. Int J Robust Nonlin Contr, 2017, 27: 2824–2841
5 Chu Z Y, Di J, Cui J. Analysis of the effect of attachment point bias during large space debris removal using a tethered space tug. Acta Astronaut, 2017, 139: 34–41
6 Guo D, Sun F, Liu H, et al. A hybrid deep architecture for robotic grasp detection. In: Proceedings of the IEEE International Conference on Robotics and Automation (ICRA), Singapore, 2017. 1609–1614
7 Liu H, Liu Y, Huang L, et al. Discovery of topical object in image collections. In: Proceedings of the IEEE International Conference on Robotics and Automation (ICRA), Seattle, 2015. 1886–1892
8 Liu H, Wu Y, Sun F, et al. Multi-label tactile property analysis. In: Proceedings of the IEEE International Conference on Robotics and Automation (ICRA), Singapore, 2017. 366–371
9 Guo D, Kong T, Sun F, et al. Object discovery and grasp detection with a shared convolutional neural network. In: Proceedings of the IEEE International Conference on Robotics and Automation (ICRA), Stockholm, 2016. 2038–2043
10 Tiwana M I, Shashank A, Redmond S J, et al. Characterization of a capacitive tactile shear sensor for application in robotic and upper limb prostheses. Sensors Actuators A Phys, 2011, 165: 164–172
11 Luo M, Sun F, Liu H. Dynamic T-S fuzzy systems identification based on sparse regularization. Asian J Contr, 2015, 17: 274–283
12 Ma R, Liu H P, Sun F C, et al. Linear dynamic system method for tactile object classification. Sci China Inf Sci, 2014, 57: 120205
13 Asif U, Iqbal J. On the improvement of multi-legged locomotion over difficult terrains using a balance stabilization method. Int J Adv Robotic Syst, 2012, 9: 1
14 Hogan N. Impedance control: an approach to manipulation-part I: theory; part II: implementation; part III-applications. J Dyn Sys Meas Control, 1985, 107: 17–24
15 Xu Q. Robust impedance control of a compliant microgripper for high-speed position/force regulation. IEEE Trans Ind Electron, 2015, 62: 1201–1209
16 Li M, Hang K, Kragic D, et al. Dexterous grasping under shape uncertainty. Robot Auton Syst, 2016, 75: 352–364
17 Stanisic R Z, Fernández V. Adjusting the parameters of the mechanical impedance for velocity, impact and force control. Robotica, 2012, 30: 583–597
18 Yoon J, Manurung A, Kim G S. Impedance control of a small treadmill with sonar sensors for automatic speed adaptation. Int J Contr Automat Syst, 2014, 12: 1323–1335
19 Petković D, Issa M, Pavlović N D, et al. Adaptive neuro fuzzy controller for adaptive compliant robotic gripper. Expert Syst Appl, 2012, 39: 13295–13304
20 Buchli J, Stulp F, Theodorou E, et al. Learning variable impedance control. Int J Robotics Res, 2011, 30: 820–833
21 Li M, Bekiroglu Y, Kragic D, et al. Learning of grasp adaptation through experience and tactile sensing. In: Proceedings of the IEEE/RSJ International Conference on Intelligent Robots and Systems(IROS), Chicago, 2014. 3339–3346
22 Jiang Y, Jiang Z P. Computational adaptive optimal control for continuous-time linear systems with completely unknown dynamics. Automatica, 2012, 48: 2699–2704

23 Johansson R, Spong M W. Quadratic optimization of impedance control. In: Proceedings of IEEE International Conference of Robotics and Automation (ICRA), San diego, 1994. 616–621
24 Xu B, Zhang P. Composite learning sliding mode control of flexible-link manipulator. Complexity, 2017, 3: 1–6
25 He W, Dong Y. Adaptive fuzzy neural network control for a constrained robot using impedance learning. IEEE Trans Neural Netw Learn Syst, 2017, 99: 1–13
26 He W, Dong Y, Sun C. Adaptive neural impedance control of a robotic manipulator with input saturation. IEEE Trans Syst Man Cybern Syst, 2016, 46: 334–344
27 Kim B, Park J, Park S, et al. Impedance learning for robotic contact tasks using natural actor-critic algorithm. IEEE Trans Syst Man Cybern B, 2010, 40: 433–443
28 Xu B, Zhang P. Minimal-learning-parameter technique based adaptive neural sliding mode control of MEMS gyroscope. Complexity, 2017, 12: 1–8
29 Ge S S, Li Y, Wang C. Impedance adaptation for optimal robot-environment interaction. Int J Contr, 2014, 87: 249–263
30 Chu Z Y, Lai M, Yan S. Optimization design of spring stiffness for under-actuated gripper (in Chinese). Acta Aeronautica Astronautica Sin, 2018, 39: 421370
31 Liu Y J, Ding F. Convergence properties of the least squares estimation algorithm for multivariable systems. Appl Math Model, 2013, 37: 476–483
32 Chu Z Y, Yan S B, Hu J, et al. Impedance identification using tactile sensing and its adaptation for an underactuated gripper manipulation. Int J Control Autom Syst, 2018, 16: 875–886